Highlights

- Skate chondroitin sulfate (sCS) production generated a by-product (BP-sCS)
- BP-sCS is a mixture of CS, type II collagen peptides, and non-collagenous peptides
- BP-sCS displayed antioxidant activity and protected fibroblasts from oxidative stress
- BP-sCS promoted fibroblast proliferation and activated collagen deposition
- BP-sCS could be a superior healing promoter of chronic wounds

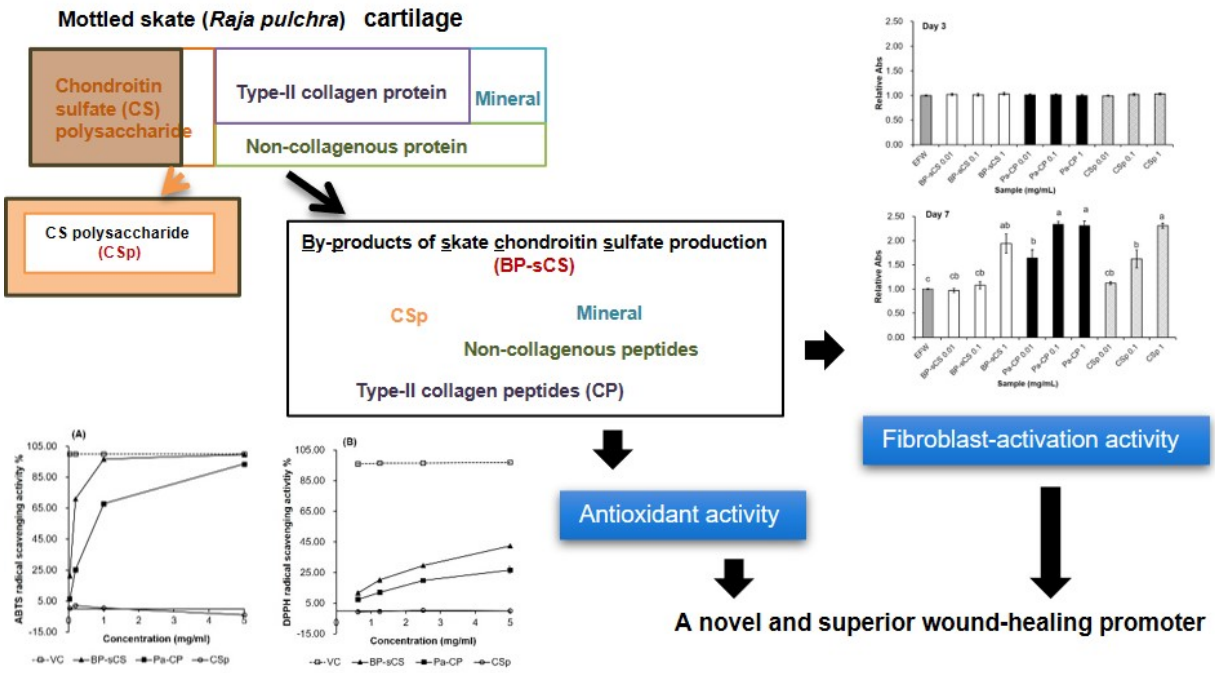
Mottled skate (Raja pulchra) cartilage
Chondroitin sulfate (CS) polysaccharide
Type-II collagen protein
Mineral
Non-collagenous protein
CS polysaccharide (CSp)
By-products of skate chondroitin sulfate production (BP-sCS)
CSp
Mineral
Non-collagenous peptides
Type-II collagen peptides (CP)
Day 3
Day 7
Relative Abs
Sample (mg/mL)
Fibroblast-activation activity
Antioxidant activity
A novel and superior wound-healing promoter
(A)
(B)
ABTS radical scavenging activity %
DPPH radical scavenging activity %
Concentration (mg/ml)
VC
BP-sCS
Pa-CP
CSp

Antioxidant and fibroblast-activating activities of the by-product of skate chondroitin extractive production

Wen Li[a]*, Naoya Terauchi[a], Dawei Meng[a,b], Nobuyuki Miyamoto[c], Naonobu Tsutsumi[d], Kazuhiro Ura[e], Yasuaki Takagi[e]

[a] *Graduate School of Fisheries Sciences, Hokkaido University, 3-1-1 Minato-Cho, Hakodate, Hokkaido 041-8611, Japan*

[b] *Zhejiang Province Joint Key Laboratory of Aquatic Products Processing, Institute of Seafood, Zhejiang Gongshang University, Hangzhou, China*

[c] *Marukyo Bio Foods, 4-18-18 Chuo, Wakkanai, Hokkaido 097-0022, Japan*

[d] *Sapporo Fine Chemical Research Center, Marukyo Bio Foods, Nishimiyanosawa 4-2-1-40, Teine, Sapporo, Hokkaido 006-0004, Japan*

[e] *Faculty of Fisheries Sciences, Hokkaido University, 3-1-1 Minato-Cho, Hakodate, Hokkaido 041-8611, Japan*

E-mail: fenzhongbahe@outlook.com (W. Li), naoya19950728708@eis.hokudai.ac.jp (N. Terauchi), dawei@mail.zjgsu.edu.cn (D. Meng), miyamoto@mbf-net.com (N. Miyamoto), naonobu_tsutsumi@mbf-net.com (N. Tsutsumi), kazu@fish.hokudai.ac.jp (K. Ura), and takagi@fish.hokudai.ac.jp (Y. Takagi)

*Corresponding author:

Wen Li, Graduate School of Fisheries Sciences, Hokkaido University, 3-1-1 Minato-Cho, Hakodate, Hokkaido 041-8611, Japan

Email: fenzhongbahe@outlook.com

Tel./fax: +81 138 40 5551

Abstract

Owing to the increasing popularity of chondroitin sulfate (CS) for joint pain treatment, the CS-production industry has been producing an increasing amount of waste, which includes type II collagen, non-collagenous proteins, and residual CS. To effectively utilize these resources, we intended to develop new products from the by-product of skate chondroitin sulfate production (BP-sCS). In this study, we examined the antioxidant and fibroblast-activating properties of BP-sCS, intending to apply it for a wound-healing promoter. BP-sCS exhibited ABTS and DPPH radical scavenging activities, protected L929 fibroblasts from H_2O_2- or AAPH-induced oxidative stress, and scavenged intracellular reactive oxygen species. Moreover, BP-sCS promoted L929 fibroblast proliferation/metabolism and stimulated collagen deposition into the extracellular matrix. In addition, BP-sCS counteracted AAPH-induced oxidative stress damage that inhibited fibroblast migration. These effect were attributed to the cooperation among the molecules of BP-sCS, namely, type II collagen peptides, non-collagenous peptides, and CS polysaccharides. Our findings indicate that BP-sCS has the potential as a novel wound-healing promoter. This study is the first step toward the realization of a sustainable CS-production industry by waste utilization in healthcare products.

Keywords: by-product, wound-healing promoter, type II collagen peptide, chondroitin sulfate polysaccharide

Abbreviations: AAPH, 2,2'-azobis(2-methylpropionamidine) dihydrochloride; ABTS, 2,2'-azino-bis(3-ethylbenzothiazoline-6-sulfonic acid; BP-sCS, the by-product of skate

52 chondroitin sulfate production; CP, collagen peptide; CS, chondroitin sulfate; DCFH,

53 dichlorofluorescein; DPPH, 2,2-diphenyl-1-picrylhydrazyl; Pa-CP, papain-hydrolyzed CP;

54 CSp, CS polysaccharides; MW, molecular weight; ROS, reactive oxygen species

55

56 **1. Introduction**

57 Chondroitin sulfate (CS) is a polysaccharide chain consisting of a repeated disaccharide
58 unit, which comprises glucuronic acid and N-acetylgalactosamine. CS is used as a
59 symptomatic slow-acting drug in Europe and a dietary supplement in the United States
60 (Volpi, 2007) for joint pain treatment. Currently, CS is extracted and purified from animal
61 cartilaginous tissues. Although microbial production, as in the case of hyaluronic acid, is an
62 attractive technology in the future (Restaino et al., 2017), it is still a challenge (Schiraldi et
63 al., 2012). Thus, industrial CS production uses cartilage sources derived from terrestrial or
64 marine animals; however, a large amount of the cartilage residue, including type II collagen,
65 non-collagenous proteins, and residual CS, is wasted during CS extraction and purification.
66 Due to the aging population and the discovery of new CS bioactivities, such as anti-obesity
67 (Li et al., 2019) and antiviral (Vázquez et al., 2013) activities and intestinal microbiota
68 modulation (Shang et al., 2016), the demand for CS production has rapidly increased
69 (Restaino et al., 2019; Vázquez et al., 2013). This, in turn, rapidly increased the waste
70 generated from CS production. To realize sustainable development and maximize profit, the
71 generated waste must be utilized. However, the utilization of the CS production waste has not
72 been demonstrated to date.

73 Generally, cartilage proteins are hydrolyzed during CS purification; therefore, the by-
74 product of CS production contains a mixture of molecules, such as CS polysaccharide
75 residues, type II collagen peptides, and non-collagenous peptides, alongside a small number
76 of minerals that bind to CS. Since CS polysaccharides and peptides with a high molecular
77 weight (MW) exhibit low absorbability in the skin and digestive system (Li et al., 2015;

78 Shang et al., 2016; Shen & Mastsui, 2017), we hypothesized that the by-product could be
79 used for wound healing as they can directly get in contact with the wound site. CS has been
80 reported to activate fibroblasts and their migration during wound healing (Zou et al., 2009),
81 while peptides, especially collagen peptides, exhibit several biological activities, such as
82 antioxidant activity, antimicrobial activity, and extracellular matrix synthesis activation (Pal
83 & Suresh, 2016). Consequently, it is possible that the by-product of CS production, which is
84 the waste now, may promote wound healing.

85 Wound healing is a complex and highly regulated process divided into three phases:
86 hemostasis and inflammation, proliferation, and remodeling (Broughton et al., 2006; Han &
87 Ceilley, 2017). Failure to progress through these normal stages of healing results in chronic
88 wounds, such as diabetic wounds and pressure ulcers (Dhivya et al., 2015; Han & Ceilley,
89 2017). An essential feature of these wounds is oxidative stress, which is caused by
90 inflammatory cells in wound tissues that produce large amounts of reactive oxygen species
91 (ROS), pro-inflammatory cytokines, and oxidases (Kurahashi & Fujii, 2015; Schäfer &
92 Werner, 2008). Although low ROS levels are required for defense against invading pathogens
93 and modulating signaling molecules, excessive ROS levels cause cellular apoptosis in the
94 surrounding tissues and imbalanced redox homeostasis, resulting in chronic wounds
95 (Kurahashi & Fujii, 2015; Schäfer & Werner, 2008). Chronic wounds are an important global
96 health problem that causes significant discomfort and distress to patients. Even in the
97 developed countries, almost 1.5% of the population experiences problematic wounds,
98 accounting for 2%–4% of all healthcare expenses (Ahmed et al., 2019). Thus, the market
99 demands superior wound-healing promoters that can achieve rapid healing at a reasonable

100 cost.

101 In northern Hokkaido, Japan, skate fishery is one of the essential industries. From the
102 newest governmental data of the aquatic product market, the total skate catch of Hokkaido is
103 1798 tons in 2018. As only their fins (about 33% of wet weight, unpublished observation) are
104 used as foods, a massive volume of cartilaginous by-products is generated from skate
105 processing. Our preliminary survey revealed that 1 ton of CS is produced per year from 270
106 tons of by-products obtained from 400 tons of skate. Thus, still, a considerable number of by-
107 products are being discarded even after CS production. Transforming this waste into value-
108 added products can mitigate environmental pollution, improve the economic profit of fishery
109 and aquaculture industries, and contribute to the circular economy in Hokkaido.

110 This study obtained a by-product of the final stage of skate CS production (BP-sCS) and
111 examined its bioactivities as a wound-healing promoter. During the proliferative phase of
112 wound healing, fibroblasts migrate to the wound site from surrounding tissues, become
113 activated, proliferate, synthesize extracellular matrix, and finally differentiate into
114 myofibroblasts to close the wound (Broughton et al., 2006). At the same time, excessive ROS
115 must be detoxified during chronic wound healing. Therefore, we focused on the antioxidant
116 and fibroblast-activating roles of BP-sCS. In addition, we examined the activities of pure CS
117 polysaccharides and type II collagen peptides to determine the active components of BP-sCS.
118 This study is the first step toward a sustainable CS production industry as our results indicate
119 that CS production wastes can be used in various healthcare products.

120 **2. Materials and methods**

121 *2.1. Materials*

122 Skate cartilage, chondroitin sulfate polysaccharide (CSp), and BP-sCS were supplied by
123 Marukyo Bio Foods (Wakkanai, Hokkaido, Japan). CSp was isolated and purified from the
124 cartilage of *Raja pulchra* (skate), and the remaining material was spray-dried to produce BP-
125 sCS containing CSp (14%), type II collagen peptides (60%), non-collagenous peptides (14%),
126 minerals (8%), and other materials (Supplementary Fig. 1, Japan Food Analysis Center
127 no.17091776001-0101). CSp was obtained as a CS sodium salt, which includes CS (83.1%)
128 and sodium (16.9%). Thus, the content of CSp in BP-sCS as CS sodium salt was 22%. Type
129 II collagen was purified from skate cartilage largely according to the method described by
130 Meng et al. (2019). The papain-hydrolyzed collagen peptides (Pa-CP) were prepared by
131 hydrolyzing the purified type II collagen using papain (2.5% w/w) at 50 °C for 4 h. The
132 formulations and molecular weight of CSp are presented in Supplementary Table 1. No
133 keratan sulfate existed in the cartilage glycosaminoglycan of most skate species (Murado et
134 al., 2010).

135 *2.2. Antioxidant assays*

136 *2.2.1. ABTS radical scavenging assay*

137 ABTS (7 mM; Wako Pure Chemical, Osaka, Japan) and potassium persulfate ($K_2S_2O_8$,
138 2.45 mM; Wako Pure Chemical) solutions (2:1 v/v) were reacted in the dark at room
139 temperature (21 °C–23 °C) for 12–16 h to generate ABTS radical solution. The solution was
140 diluted with phosphate-buffered saline (PBS, pH 7.4) to an absorbance of 0.70 ± 0.02 at 734

141 nm, reacted (500 μL) with 500 μL of sample solution for 10 min at room temperature (21 °C–
142 23 °C), and the absorbance determined at 734 nm using a microplate reader (Infinite F50R,
143 Tecan Japan, Kanagawa, Japan). Each sample was dissolved in deionized water to
144 concentrations of 0.04–5 mg/mL. L (+)-ascorbic acid (VC, Wako Pure Chemical) was used as
145 the positive control. Each measurement was performed in triplicate, and the percentage of the
146 scavenging effect was calculated as follows:

147 $$\text{ABTS radical scavenging activity (\%)} = (A_b - A_s)/A_b \times 100,$$

148 where A_b and A_s denote the absorbance of deionized water and sample solution, respectively.

149 *2.2.2. DPPH radical scavenging assay*

150 DPPH (Tokyo Chemical Industry, Tokyo, Japan) was dissolved in methanol at a
151 concentration of 115 μM. Each sample was dissolved in deionized water at concentrations of
152 0.625–5 mg/mL. VC was used as a positive control. Next, the sample solution (500 μL) was
153 reacted with DPPH methanol solution (500 μL) in the dark at room temperature (21 °C–23
154 °C) for 30 min, and the absorbance was measured at 517 nm using a microplate reader
155 (Infinite F50R, Tecan Japan, Kawasaki, Japan). Each measurement was performed in
156 triplicate, and the percentage of the scavenging effect was calculated as follows:

157 $$\text{DPPH radical scavenging activity (\%)} = (A_b - A_s)/A_b \times 100,$$

158 where A_b and A_s denote the absorbance of deionized water and sample solution, respectively.

159 *2.3. Molecular weight distribution of peptides*

160 Peptides and CSp residues in the BP-sCS were separated *via* ultrafiltration using the

161 molecular weight cutoff (MWCO) of 3000 and 10000 Da (Merck Millipore, Darmstadt,
162 Germany). A 5-mL aliquot of BP-sCS solution was firstly centrifuged at 4,000 × *g* for 20 min
163 and then eluted with 5-mL deionized water at 4,000 × *g* for 20 min using a filter with an
164 MWCO of 10000 Da. The elution process was repeated several times to obtain <10000 Da
165 fraction. Then, the <10000 Da fraction was separated into 10000–3000 Da and <3000 Da
166 fractions using a filter with an MWCO of 3000 Da. Since the MW of the CSp in BP-sCS is
167 much larger than 3000 Da (Supplementary Fig. 1B), the <3000 Da fraction of BP-sCS did not
168 contain CS (Supplementary Fig. 1C). However, the separation also excluded peptides larger
169 than 3000 Da in BP-sCS. Therefore, the <3000 Da fraction of Pa-CP was obtained to
170 compare its bioactivity with the <3000 Da fraction of BP-sCS. The collected fractions were
171 freeze-dried. The MW distribution of the <3000 Da fractions was determined *via* size
172 exclusion chromatography using a TSKgel G2500PW column (7.5 mm × 30 cm, Tosoh,
173 Tokyo, Japan) with UV detection at 214 nm and a mobile phase of 35% acetonitrile in 0.05%
174 TFA (pH 2.1) at a flow rate of 0.6 mL/min. An MW calibration curve was obtained using the
175 following standards: insulin (5700 Da), vitamin B_{12} (1355 Da), and triglycine (189 Da). A 30-
176 μL aliquot of each sample or standard was analyzed using High Performance Liquid
177 Chromatography system (HPLC, SCL-10AVP, Shimadzu, Tokyo, Japan), and the percentage
178 of each MW fraction was calculated as follows:

179 $$\text{MW fraction (\%)} = (S_x/S_{total}) \times 100,$$

180 where S_x and S_{total} denote the area of each fraction (>5000 Da, 3000–5000 Da, 1000–3000
181 Da, and <1000 Da) and the total area of the chromatogram, respectively.

182 *2.4. Cell culture experiments*

183 *2.4.1 Cell culture condition*

184 L929 fibroblast cells from the RIKEN Cell Bank (Tsukuba, Japan) was cultured at 37 °C
185 with 5% CO_2 in the minimum essential medium (MEM, Gibco, Grand Island, NY, USA)
186 containing 1% penicillin/streptomycin (Thermo Fisher Scientific, Waltham, MA) with 5%
187 fetal bovine serum (FBS, Lot. No 451456, Gibco). The medium was changed every 2–3 d.
188 The samples dissolved in endotoxin-free water (EFW) were added to the culture medium at
189 various concentrations for different experiments, and EFW was used as a negative control.
190 The endotoxin levels in MEM and the samples (1 mg/mL) were less than 1.0 EU/mL.

191 *2.4.2. Antioxidant assay in cell culture*

192 Cell viability/activity assay under oxidative stress was performed using the strong
193 oxidant H_2O_2 (Wako Pure Chemical) and the weak oxidant AAPH (Tokyo Chemical
194 Industry). Briefly, L929 cells were seeded in each well of a 96-well plate (2×10^3 cells/well).
195 When the cells reached >90% confluency, samples were added to the culture medium to
196 produce a final concentration of 1 mg/mL. After 24 h, the cells were exposed to H_2O_2 (0.5
197 mM) or AAPH (5 mM) and incubated for another 24 h. After incubation, the cells were
198 washed with the Hank's balanced salt solution (HBSS, Sigma-Aldrich, Saint Louis, MO,
199 USA), and cell viability was assessed using Cell Counting Kit-8 (CCK-8, Dojindo,
200 Kumamoto, Japan), which measures the total metabolic activity. For the assay, the culture
201 medium was replaced with that containing 10% (v/v) CCK-8, and the cells were incubated at
202 37 °C for 30 min, and the absorbance at 450 nm was measured using a microplate reader

203 (Infinite F50R, TECAN, Kawasaki, Japan). This assay was also used to estimate the total cell
204 number in the well to evaluate cell proliferation; this measurement postulates that the
205 metabolism of each cell remains constant during the assay. As we cannot ascertain whether
206 the cell metabolism was affected by the addition of samples, the term
207 "proliferation/metabolism" was used for the measurements of cell proliferation assessed in
208 this experiment. The data were expressed as the relative absorbance normalized to that of the
209 control well (no oxidant).

210 Intracellular ROS formation was assessed according to the method described by Ahn et
211 al. (2012) with minor modifications. The oxidation-sensitive dye H_2DCFDA was used as a
212 probe as it diffuses through the cell membrane and is hydrolyzed into its nonfluorescent form
213 dichlorofluorescein (DCFH) by intracellular esterase. Then, DCFH reacts with the
214 intracellular H_2O_2 to produce an oxidized form of DCFH, which is a green fluorescent dye.
215 L929 cells (2×10^3 cells/well) were grown in a black/transparent 96-well microtiter plate
216 until they reached >90% confluency and were treated with the samples for 24 h. After
217 discarding the culture medium, the cells were washed with HBSS and labeled with
218 H_2DCFDA (20 μM; Sigma-Aldrich) in HBSS for 20 min in the dark at 37 °C and then
219 washed with HBSS and incubated with 0.5 mM H_2O_2 in HBSS for 30 min in the dark at 37
220 °C. Fluorescence was read at an excitation wavelength of 485 nm and an emission
221 wavelength of 528 nm using a fluorescence microplate reader (WallAc ARVO 1420
222 Multilabel Counter, PerkinElmer, Waltham, MA, USA). VC was used as a positive control.
223 Data have been expressed as the relative fluorescence intensity normalized to that of the
224 control well (no oxidant).

225 *2.4.3. Fibroblast proliferation/metabolism and collagen production*

226 L929 cells (5×10^3 cells/well) were seeded in a 48-well plate. After 24 h, the culture
227 medium was replaced with a medium containing 1-mg/mL sample (Day 0). Fibroblast
228 proliferation was assessed based on a method described by Li et al. (2019) using the CCK-8
229 assay. Then, type I collagen gene expression was analyzed *via* real-time quantitative PCR
230 (qPCR). Total RNA was extracted from each well using the ISOGEN II reagent (Nippon
231 Gene, Tokyo, Japan) and quantified using a spectrophotometer (ND-1000, Thermo Fisher
232 Scientific, Waltham, MA, USA). cDNA was synthesized from 500 ng total RNA using a
233 PrimeScript RT Reagent Kit with the gDNA Eraser Perfect Real Time (Takara Holdings,
234 Ohtsu, Japan), according to the manufacturer's instructions. qPCR was performed using a
235 real-time PCR system (LightCycler® Nano System, Basel, Switzerland) with the synthesized
236 cDNA, which was diluted five times, as the template. Amplification was performed at a final
237 volume of 15 μL, containing 1 μL of the cDNA template, 7.5 μL of 2X SYBR (FastStart
238 Universal SYBR Green Master, Roche, Basel, Switzerland), 1.5 μL of each primer (5 μM
239 each), and 3.5 μL of sterilized water. PCR was performed as follows: 95 °C for 10 min,
240 followed by 40 cycles of 95 °C for 10 s, 56 °C for 10 s, and 72 °C for 15 s. The reaction used
241 primers for the type I procollagen α1 gene *Col1a1* (COL1A1-F: 5′-AAC CCG AGG TAT
242 GCT TGA TCT-3′ and COL1A1-R: 5′-CCA GTT CTT CAT TGC ATT GC-3′) and *Gapdh*
243 (GAPDH-F: 5′-TCC CAC TCT TCC ACC TTC-3′ and GAPDH-R: 5′-CTG TAG CCG TAT
244 TCA TTG TC-3′) (Kanazawa et al., 2008; Yoshimoto et al., 2009). Relative gene expression
245 was calculated using the $2^{-\Delta\Delta CT}$ method with *Gapdh* as the internal control (Schmittgen &
246 Livak, 2008). Data have been expressed as relative values normalized based on the control

247 well (EFW only).

248 Collagen production was quantified by the Sircol™ Soluble Collagen Assay (Biocolor
249 Ltd., Carrickfergus, Northern Ireland, UK) according to the manufacturer's instruction. In
250 this experiment, L929 cells (1.2×10^4 cells/well) were seeded in 24-well plates. The culture
251 medium was sampled on Days 3 and 6 to measure the collagen content in the medium. On
252 Day 3, a new culture medium was added after the sampling. On Day 6, 0.1 mg/mL pepsin in
253 0.5 M acetic acid was added after the sampling of the medium, and the wells were incubated
254 overnight at 4 °C to extract collagen from the extracellular matrix (ECM) secreted by L929
255 cells during the culture. In the ECM, collagen molecules assembled into fibrils and became
256 insoluble. Pepsin can remove the terminal non-helical telopeptides of collagen molecules to
257 release them into the extract. Prior to the assay, the samples were concentrated using the
258 isolation and concentration reagent provided in the kit. In the case of the extracted samples,
259 those from three wells were mixed to make one test-sample as the collagen concentration was
260 low. Then, the collagen concentrations were quantified using a Sircol assay kit according to
261 the manufacturer's instructions. The collagen test was conducted in triplicate for each sample.
262 The amount of soluble collagen secreted into the culture medium was obtained as the sum of
263 collagen in the media on Days 3 and 6.

264 *2.4.4. Fibroblast migration*

265 To assess the effects of BP-sCS on the migration of fibroblasts, the scratch assay was
266 conducted using the methods described by Liang et al. (2007) with minor modifications.
267 Briefly, L929 cells (1.2×10^4 cells/well) were seeded in 24-well plates with a reference point

268 in each well, and when the cells reached confluence, a scratch through the reference point in
269 the cell monolayer was generated using a sterile 200-μL pipette tip. The wells were washed
270 with HBSS to remove debris, and the culture medium containing each sample was added. For
271 the scratch-oxidative stress tests, AAPH was added to the culture medium at a final
272 concentration of 5 or 2.5 mM (Alvarez-Suarez et al., 2016).

273 The scratch was gradually occupied with the fibroblasts migrating from the non-scratched
274 area during the culture. Thus, time-course changes on the area of each scratch were observed
275 and photographed under a microscope (DMI600B, Leia, Wetzlar, Germany), and the images
276 obtained for each well were quantitatively analyzed using the ImageJ software (1.52a,
277 National Institutes of Health, USA). In brief, the scratch was defined as the region of interest,
278 and its area was measured using the software. The fibroblast-migration activity was assessed
279 as the repair rate (percentage scratch closure) calculated as follows:

280 $$\text{Repair rate (\%)} = [\text{area (0 h)} - \text{area } (x \text{ h})]/\text{area (0 h)} \times 100,$$

281 where area (0 h) and area (x h) indicate the scratch area at time 0 and time x (x = 6, 12, 24,
282 30, and 36 h), respectively.

283 *2.5. Statistical analyses*

284 Data have been expressed as the mean ± standard error. Statistical analyses were
285 conducted using Student's *t*-test, Dunnett's test, or the Steel-Dwass test after ANOVA with
286 the Microsoft Excel add-in statistical software (SSRI, Tokyo, Japan).

287 **3. Results and discussion**

288 *3.1. Antioxidant activity of BP-sCS*

289 *3.1.1 Free-radical scavenging activity*

290 We examined the antioxidant activity of BP-sCS using ABTS and the DPPH scavenging
291 assays and found that BP-sCS exhibited a strong antioxidant activity, particularly in the
292 ABTS radical scavenging assay (Fig. 1A). At concentrations over 1 mg/mL, BP-sCS was able
293 to scavenge almost all the ABTS radicals, which was the same as VC. Although CSp
294 displayed no activity in the DPPH or ABTS assays, Pa-CP was able to scavenge radicals in a
295 dose-dependent manner; therefore, type II CP, not CSp, is one of the critical antioxidant
296 components in BP-sCS.

297 Next, we separated CSp and the peptides in BP-sCS using a 3000 Da MWCO
298 ultrafiltration membrane. Tricine-SDS-PAGE revealed that the <3000 Da fraction of BP-sCS
299 contained only peptides (Supplementary Fig. 1C), which may include type II CP and non-
300 collagenous peptides. Similarly, we separated the <3000 Da fraction of Pa-CP and compared
301 the ABTS radical scavenging activity of the <3000 Da BP-sCS and Pa-CP fractions (1
302 mg/mL). Antioxidant activity was significantly higher in the <3000 Da BP-sCS fraction than
303 that in Pa-CP (Fig. 2A), suggesting that non-collagenous peptides in BP-sCS contribute to its
304 antioxidant activity.

305 Further, we analyzed the MW distribution of the <3000 Da BP-sCS and Pa-CP fractions
306 *via* size exclusion chromatography (Fig. 2B) and found that BP-sCS contained more
307 <1000 Da peptides and less 3000–5000 Da peptides than Pa-CP. Membrane retention depends
308 not only on the solute's molecular size but also on its shape. The MWCO membrane cannot

309 fully reject the molecules whose MW is above their nominal MWCO (Sun et al., 2011).
310 Therefore, the <3000 Da fractions of BP-sCS included 3000–5000 Da peptides. Many studies
311 have reported that peptides with a lower MW exhibit a stronger antioxidant activity (Agrawal
312 et al., 2019; Nwachukwu & Aluko, 2019; Zou et al., 2016), and it has been suggested that
313 smaller peptides may expose more bioactive fragments *via* hydrolysis (Zou et al., 2016).
314 Therefore, the peptides with a lower MW in BP-sCS may also be responsible for its high
315 antioxidant activity.

316 *3.1.2 Protection of cells from oxidative stress*

317 H_2O_2 generates free radicals; thus, it is commonly used to induce cell death and study
318 oxidative stress (Canas et al., 2007). In this study, we established an H_2O_2-induced oxidative
319 stress model (Fig. 3A), in which the addition of 0.5 mM H_2O_2 significantly reduced cell
320 viability/activity to approximately 70% that of the control cells, as quantified by the CCK-8
321 assay. Treating cells with 1 mg/mL of BP-sCS significantly reduced the H_2O_2-induced
322 damage, increasing their viability/activity to approximately 50% that of the control cells. Pa-
323 CP demonstrated a smaller protective effect than BP-sCS, and the treatment with CSp did not
324 affect cell viability/activity.

325 We also produced another oxidative stress model using AAPH, which initiates free-
326 radical reactions by generating radicals at a constant rate of 37 °C. Thus, AAPH acted more
327 slowly and had gentler effects than H_2O_2. AAPH (5 mM) treatment for 24 h reduced the cell
328 viability to approximately 50% that of the control group, which was gentler than the H_2O_2
329 treatment (70%) (Fig. 3B). Treatment with BP-sCS or Pa-CP significantly increased the cell

330 viability/activity compared with that in the EFW group. CSp was again ineffective. Taken
331 together, the results from the H_2O_2 and AAPH models indicate that peptides, but not CSp,
332 were the major compounds in BP-sCS, which have significant cytoprotective activities
333 against oxidative stress. This is consistent with the previous studies in which peptides derived
334 from the tilapia skin, lantern fish hydrolysate, and microalgae were found to exert
335 cytoprotective effects under AAPH- and H_2O_2-induced oxidative stresses (Chai et al., 2016;
336 Zeng et al., 2018; Zheng et al., 2018). Davalos et al. (2004) reported that among the amino
337 acids, tryptophan, tyrosine, and methionine exhibited the highest antioxidant activity,
338 followed by cysteine, histidine, and phenylalanine. Glycine and proline also play significant
339 roles in the antioxidant activity of peptides (Li et al., 2017). Thus, the antioxidant activity
340 must be the common biological activity of peptides, and the activity seems to be based on
341 their amino acid sequence. In addition, BP-sCS contained more <1000 Da peptides and less
342 3000–5000 Da peptides than Pa-CP (Fig. 2B). Therefore, the peptides with a lower MW in
343 BP-sCS, which may expose more bioactive fragments, has a higher potency of antioxidant
344 activity.

345 *3.1.3 Reduction of intracellular ROS production*

346 Next, we examined whether the compounds in BP-sCS could reduce H_2O_2-induced
347 intracellular ROS production using a fluorescent probe, whose fluorescence increases as free
348 radicals are generated within a cell (Ahn et al., 2012). Exposing L929 cells to 0.5 mM H_2O_2
349 significantly increased the intracellular ROS production (Fig. 4), whereas the ROS
350 production was significantly reduced when the cells were treated with the positive control

351 (VC) or 1 mg/mL of BP-sCS. The same concentration of Pa-CP and CSp could prevent
352 intracellular ROS production, although they exhibited no significant cell-protective effects
353 against H_2O_2-induced oxidative stress.

354 Cellular antioxidant enzymes can deactivate intracellular ROS before they attack cellular
355 components and maintain cellular redox homeostasis (Tao et al., 2018). Non-collagenous
356 peptides and CS-A from cartilage have been reported to increase the intracellular levels of
357 antioxidant enzymes under oxidative stress (Canas et al., 2007; Tao et al., 2018). CS-A is the
358 second major component and occupies 26.6% of the skate CS (Supplementary Table 1).
359 Therefore, BP-sCS could regulate the antioxidant enzymes, at least in part, through its CS-A
360 and non-collagenous peptides and reduce intracellular ROS. Although the relationships
361 between type II CP and antioxidant enzymes remain unclear, the collagen hydrolysate from
362 Nile tilapia skin (type I CP) enhanced the activities of antioxidant enzymes to alleviate
363 oxidative stress (Wang et al., 2018). Thus, we believe that type II CP also influences
364 antioxidant enzymes.

365 In these experiments, the sample-containing culture medium had already been changed
366 to that without samples before H_2O_2 was added; thus, peptides and CS may have been
367 transported into cells *via* cell surface transporters or membrane channels to exert their
368 antioxidant activities. Alternatively, they may have bound cell surface receptors to produce
369 intracellular effects. Several peptide transporters (PEPTs) and CS receptors have been
370 reported. For instance, PEPT-1 was found to be involved in the cellular uptake of peptides in
371 skin keratinocytes (Kudo et al., 2016). Moreover, Zheng et al. (2018) reported that fish skin
372 peptides failed to inhibit ROS production in H_2O_2-exposed porcine enterocytes with PEPT1

373 knockdown. In addition, CS chain receptors, such as Toll-like receptor 2 and annexin 6, have
374 been identified on the surface of fibroblasts (Takagi et al., 2002; Wu et al., 2018). These
375 studies strongly suggest that the antioxidative effects of BP-sCS depend on transporter- and
376 receptor-related signaling pathways.

377 *3.2. Effect of BP-sCS on L929 fibroblast activity*

378 *3.2.1 Fibroblast proliferation/metabolism*

379 To evaluate their effect on fibroblast proliferation/metabolism, L929 cells were treated
380 with 0.01 mg/mL, 0.1 mg/mL, or 1 mg/mL of BP-sCS, Pa-CP, or CSp for up to 7 d (Fig. 5).
381 No significant effects were observed after 3 d (Fig. 5A); however, Pa-CP and CSp
382 significantly enhanced L929 fibroblast proliferation/metabolism in a dose-dependent manner
383 after 7 d (Fig. 5B). The lowest effective concentrations of Pa-CP and CSp were 0.01 and 0.1
384 mg/mL, respectively, whereas BP-sCS significantly activated fibroblast
385 proliferation/metabolism at 1 mg/mL. Thus, high BP-sCS concentrations promote fibroblast
386 proliferation/metabolism, and its activity is mainly due to type II CP and CSp.

387 Previously, we found that skate CS polysaccharides accelerated 3T3-L1 fibroblast
388 proliferation/metabolism (Li et al., 2019), whereas several studies have reported the fibroblast
389 proliferation activity of type I collagen-derived peptides. For example, collagen peptides
390 from the Asian sea bass were found to promote L929 fibroblast proliferation (Benjakul et al.,
391 2018), whereas those from tilapia scales were shown to stimulate human skin fibroblast
392 proliferation (Chai et al., 2010). However, this study is the first to report the effects of type II
393 peptides on fibroblast proliferation/metabolism.

394 *3.2.2 Collagen production*

395 Type I collagen is secreted by skin fibroblasts during wound healing to construct a new
396 extracellular matrix (Broughton et al., 2006). In this study, we first analyzed the type I
397 collagen α1 chain (*Col1a1*) mRNA expression. Cell proliferation assays determined the
398 effective BP-sCS dose (1000 μg/mL) for subsequent experiments. As can be seen from Figure
399 6A, BP-sCS slightly and transiently activated the *Col1a1* gene expression compared with that
400 in control. Neither Pa-CP nor CSp increased the *Col1a1* expression. These results indicate
401 that BP-sCS stimulates type I collagen synthesis at the mRNA transcriptional level, whereas
402 the minimal effect of Pa-CP and CSp suggests that the BP-sCS activity is mainly due to non-
403 collagenous peptides.

404 Next, we monitored the effects of BP-sCS on collagen production by fibroblasts in two
405 phases: the soluble collagen secreted into the culture medium and the insoluble collagen
406 incorporated into the ECM. The results indicated that BP-sCS significantly lowered the
407 soluble collagen level of the culture medium but significantly increased the collagen level in
408 the ECM (Fig. 6B). These data indicated that BP-sCS changed the distribution ratio of
409 collagen produced by fibroblasts, i.e., BP-sCS induced more collagen to deposit into the
410 ECM and less collagen to secrete into the culture medium. The cell number increased by
411 1.94-fold, and the ECM collagen levels increased by 2.83-fold in the BP-sCS group
412 compared with that in the EFW group during a week of culture (Figs. 5, 6B). This suggests
413 that the increase in ECM collagen is due to not only the cell proliferation-promoting activity
414 but also the collagen deposition-promoting activity of BP-sCS. Several previous reports have
415 demonstrated that type I CP and non-collagenous peptides increased the intracellular collagen

416 contents of fibroblasts (Zeng et al., 2018) or accelerated the secretion of collagen into the
417 culture medium by fibroblasts (Benjakul et a., 2018; Chotphruethipong et al., 2019; Pozzolini
418 et al., 2018; Zague et al., 2018). However, to the best of our knowledge, this is the first study
419 that reports the promotion of collagen deposition into the ECM. Although the precise
420 mechanism of BP-sCS that stimulates collagen deposition into the ECM is not revealed by
421 this study, non-collagenous ECM proteins, such as small leucine-rich proteoglycans, secreted
422 by fibroblasts may regulate it as they play critical roles in collagen fibrillogenesis (Taye et al.,
423 2020). The effects of BP-sCS on non-collagenous ECM proteins should be studied in the
424 future.

425 *3.2.3 Fibroblast migration*

426 The scratch assay is particularly suitable for studying cell migration during wound
427 healing (Liang et al., 2007). As presented in Figure 7A, treatment with BP-sCS, Pa-CP, or
428 CSp (1 mg/mL) tended to transiently and slightly increase L929 fibroblast migration during
429 the first 12 h, whereas the scratch healed in all groups after 24 h. Hu et al. (2017) prepared
430 peptides *via* hydrolyzation of tilapia skin type I collagen with neutral protease and papain and
431 demonstrated that the peptides significantly enhanced the migration of HaCaT keratinocytes.
432 Therefore, the different amino acid compositions and MW distributions of the peptides may
433 vary their effects on cell migration. Moreover, peptides may differently affect the migration
434 of keratinocytes and fibroblasts. In addition, Zou et al. (2009) showed pure CS-C and CS-A
435 had a migration-promoting activity of human dermal fibroblasts. CS polysaccharides
436 obtained from animal sources are a mixture of non-, mono-, and disulfated disaccharides. The

437 functionality of CS polysaccharides depends on their composition, which varies depending on
438 their species of origin (Li et al., 2019). Therefore, the difference in fibroblast migration
439 activity between the report of Zou et al. (2019) and the present study may be due to the
440 compositional differences of CS.

441 Next, we examined fibroblast migration under oxidative stress to simulate chronic
442 wound conditions. Treatment with 5-mM AAPH significantly reduced fibroblast migration
443 but was significantly counteracted by Pa-CP (Fig. 7B). A lower concentration of AAPH (2.5
444 mM) had a weaker inhibitory effect on fibroblast migration (Fig. 7C). Under this condition,
445 Pa-CP and BP-sCS stimulated fibroblast migration, although the differences were
446 insignificant. After 24 h, fibroblasts in the EFW and CSp groups started to die, and the
447 scratch site enlarged (Fig. 7C); however, the cells did not die, and the scratch did not enlarge
448 in the BP-sCS and Pa-CP groups (Fig. 7C). After 48 h, the fibroblasts in the control group (no
449 AAPH) contacted each other, and the scratch completely closed (Fig. 7D), whereas the
450 AAPH-stressed fibroblasts (EFW (AAPH) group in Fig. 7D) shrank and separated from each
451 other, which could be the result of cell contraction and reduced cell number due to oxidative
452 damage. Although the scratch in the BP-sCS and Pa-CP groups did not close, the AAPH-
453 stressed fibroblasts in these groups (BP-sCS + AAPH and Pa-CP + AAPH groups in Fig. 7D)
454 retained their normal morphology, and no further enlargement of the scratch was observed.
455 Therefore, BP-sCS may counteract the inhibitory effects of oxidative stress on fibroblast
456 migration, likely due to type II CP (Pa-CP), which significantly enhances fibroblast migration
457 under oxidative stress (Fig. 7B), consistent with the results of the antioxidant assay.
458 Excessive ROS levels are an essential feature of chronic, non-healing wounds (Schäfer &

459 Werner, 2008); therefore, the counteractivity of BP-sCS against ROS-induced loss of
460 fibroblast migration may be beneficial for chronic wound healing. A similar scratch-based
461 oxidative stress model previously demonstrated the antioxidant activity of honey, which
462 protected fibroblasts against oxidative damage and promoted fibroblast migration (Alvarez-
463 Suarez et al., 2016). This study is the first to report the activity of fish by-products on
464 fibroblast migration under oxidative stress.

465 **4. Conclusion**

466 BP-sCS, a presently wasted by-product of skate CS extraction, is a combined
467 preparation of skate CSp, type II CP, and non-collagenous peptides. It exhibits antioxidant
468 activities, protects fibroblasts from oxidative stresses, promotes fibroblast
469 proliferation/metabolism, and counteracts oxidative stress damage that inhibits fibroblast
470 migration. We also found that the type II CP and non-collagenous peptides exhibited
471 antioxidant activities, whereas CSp and type II CP showed fibroblast activating properties;
472 however, none of these purified compounds exhibited all the bioactivities of BP-sCS
473 independently. Although many studies have reported the activities and applications of CS or
474 peptides as bioactive compounds, the industrial applications of BP-sCS, involving low-cost,
475 environmentally friendly products that are uncontaminated with zoonosis pathogens and are
476 subject to no religious objections, have not been considered. These advantages make BP-sCS
477 a competitive potential bioactive compound, such as a healing promoter of chronic wounds.
478 This study is the first step toward the realization of a sustainable CS production industry
479 based on the utilization of wastes with bioactivity capabilities. However, our preliminary

estimation revealed that CS and BP-sCS occupy approximately 6% of by-products after skate processing. Although skin (10% of by-products) is used for collagen production, a large part of by-products is still not efficiently used. Further studies on the under-utilized sections of by-products will be conducted in the future.

Acknowledgments

This study was supported in part by a grant-in-aid for the Research and Development for the Recycle Technology from the Hokkaido Local Government Office. We would like to thank Editage group (www.editage.jp) for English language editing.

Declaration of interest: None

References

Agrawal, H., Joshi, R., Gupta, M., 2019. Purification, identification and characterization of two novel antioxidant peptides from finger millet (*Eleusine coracana*) protein hydrolysate. Food Res. Int. 120, 697–707.

Ahmed, T. A., Suso, H. P., Maqbool, A., Hincke, M. T., 2019. Processed eggshell membrane powder: Bioinspiration for an innovative wound healing product. Mat. Sci. Eng. C. 95, 192–203.

Ahn, C. B., Je, J. Y., Cho, Y. S., 2012. Antioxidant and anti-inflammatory peptide fraction from salmon by-product protein hydrolysates by peptic hydrolysis. Food Res. Int. 49, 92–98.

Alvarez-Suarez, J. M., Giampieri, F., Cordero, M., Gasparrini, M., Forbes-Hernández, T. Y.,

500 Mazzoni, L., Afrin, S., Beltran-Ayala, P., Gonzalez-Paramas, A. M., Santos-Buelga, C.,
501 Varela-Lopez, A., Quiles, J. L., Battion, M., 2016. Activation of AMPK/Nrf2 signalling
502 by Manuka honey protects human dermal fibroblasts against oxidative damage by
503 improving antioxidant response and mitochondrial function promoting wound healing. J.
504 Funct. Foods. 25, 38–49.
505 Benjakul, S., Karnjanapratum, S., Visessanguan, W., 2018. Hydrolysed collagen from *Lates*
506 *calcarifer* skin: its acute toxicity and impact on cell proliferation and collagen
507 production of fibroblasts. Int. J. Food Sci. Tech. 53, 1871–1879.
508 Broughton, G. 2nd, Janis, J. E., Attinger, C. E., 2006. The basic science of wound healing.
509 Plast. Reconstr. Surg. 117, 12S–34S.
510 Canas, N., Valero, T., Villarroya, M., Montell, E., Verges, J., García, A. G., Lopez, M. G.,
511 2007. Chondroitin sulfate protects SH-SY5Y cells from oxidative stress by inducing
512 heme oxygenase-1 via phosphatidylinositol 3-kinase/Akt. J. Pharmacol. Exp. Ther. 323,
513 946–953.
514 Chai, H. J., Li, J. H., Huang, H. N., Li, T. L., Chan, Y. L., Shiau, C. Y., Wu, C. J., 2010.
515 Effects of sizes and conformations of fish-scale collagen peptides on facial skin qualities
516 and transdermal penetration efficiency. J. BioMed Res. 2010, 757301.
517 Chai, H. J., Wu, C. J., Yang, S. H., Li, T. L., Pan, B. S., 2016. Peptides from hydrolysate of
518 lantern fish (*Benthosema Pterotum*) proved neuroprotective *in vitro* and *in vivo*. J. Funct.
519 Foods. 24, 438–449.
520 Chotphruethipong, L., Aluko, R. E., Benjakul, S., 2019. Hydrolyzed collagen from porcine
521 lipase-defatted seabass skin: antioxidant, fibroblast cell proliferation, and collagen

522 production activities. J. Food Biochem. 43, e12825.

523 Davalos, A., Miguel, M., Bartolome, B., Lopez-Fandino, R., 2004. Antioxidant activity of
524 peptides derived from egg white proteins by enzymatic hydrolysis. J. Food Prot. 67,
525 1939–1944.

526 Dhivya, S., Padma, V. V., Santhini, E., 2015. Wound dressings - a review. BioMed. 5, 24–28

527 Han, G., Ceilley, R., 2017. Chronic wound healing: a review of current management and
528 treatments. Adv. Ther. 34, 599–610.

529 Hu, Z., Yang, P., Zhou, C., Li, S., Hong, P., 2017. Marine collagen peptides from the skin of
530 Nile Tilapia (*Oreochromis Niloticus*): Characterization and wound healing evaluation.
531 Mar. Drugs, 15, 102–113.

532 Kanazawa, I., Yamaguchi, T., Yano, S., Yamauchi, M., Sugimoto, T., 2008. Metformin
533 enhances the differentiation and mineralization of osteoblastic MC3T3-E1 cells via AMP
534 kinase activation as well as eNOS and BMP-2 expression. Biochemi. Biophysi. Res.
535 Commun. 375, 414–419.

536 Kudo, M., Katayoshi, T., Kobayashi-Nakamura, K., Akagawa, M., Tsuji-Naito, K., 2016.
537 H^+/peptide transporter (PEPT2) is expressed in human epidermal keratinocytes and is
538 involved in skin oligopeptide transport. Biochem. Bioph. Res. Co. 475, 335–341.

539 Kurahashi, T., Fujii, J., 2015. Roles of antioxidative enzymes in wound healing. J. Dev. Biol.
540 3, 57–70.

541 Li, H., Low, Y. S. J., Chong, H. P., Zin, M. T., Lee, C. Y., Li, B., Leolukman, M., Kang, L.,
542 2015. Microneedle-mediated delivery of copper peptide through skin. Pharm. Res. 32,
543 2678–2689.

544 Li, W., Kobayashi, T., Moroi, S., Kotake, H., Ikoma, T., Saeki, H., Ura, K., Takagi, Y., 2019.
545 Anti-obesity effects of chondroitin sulfate oligosaccharides from the skate *Raja*
546 *phulchra*. Carbohyd. Polym. 214, 303–310.
547 Li, X., Chi, C., Li, L., Wang, B., 2017. Purification and identification of antioxidant peptides
548 from protein hydrolysate of scalloped hammerhead (*Sphyrna lewini*) cartilage. Mar
549 Drugs. 15, 1–16.
550 Liang, C. C., Park, A. Y., Guan, J. L., 2007. *In vitro* scratch assay: a convenient and
551 inexpensive method for analysis of cell migration *in vitro*. Nat. Protoc. 2, 329–333.
552 Meng, D., Tanaka, H., Kobayashi, T., Hatayama, H., Zhang, X., Ura, K., Yunoki, S., Takagi,
553 Y., 2019. The effect of alkaline pretreatment on the biochemical characteristics and
554 fibril-forming abilities of types I and II collagen extracted from bester sturgeon by-
555 products. Int. J. Biol. Macromol. 131, 572–580.
556 Murado, M. A., Fraguas, J., Montemayor, M. I., Vázquez, J. A., González, P., 2010.
557 Preparation of highly purified chondroitin sulphate from skate (*Raja clavata*) cartilage
558 by-products. Biochem. Eng. J., 49, 126–132.
559 Nwachukwu, I. D., Aluko, R. E., 2019. Structural and functional properties of food protein -
560 derived antioxidant peptides. J. Food Biochem. 43, e12761.
561 Pal, G. K., Suresh, P. V., 2016. Sustainable valorisation of seafood by-products: recovery of
562 collagen and development of collagen-based novel functional food ingredients. Innov.
563 Food Sci. Emerg. 37, 201–215.
564 Pozzolini, M., Millo, E., Oliveri, C., Mirata, S., Salis, A., Damonte, G., Arkel, M., Scarfì, S.,
565 2018. Elicited ROS scavenging activity, photoprotective, and wound-healing properties

566 of collagen-derived peptides from the marine sponge *Chondrosia reniformis*. Mar. Drugs
567 16, 465–491.
568 Restaino, O. F., di Lauro, I., Di Nuzzo, R., De Rosa, M., Schiraldi, C., 2017. New insight into
569 chondroitin and heparosan-like capsular polysaccharide synthesis by profiling of the
570 nucleotide sugar precursors. Biosci. Rep., 37, 1–11.
571 Restaino, O. F., Finamore, R., Stellavato, A., Diana, P., Bedini, E., Trifuoggi, M., Rosa, M.,
572 Schiraldi, C., 2019. European chondroitin sulfate and glucosamine food supplements: a
573 systematic quality and quantity assessment compared to pharmaceuticals. Carbohyd.
574 Polym. 222, 114984.
575 Schäfer, M., Werner, S., 2008. Oxidative stress in normal and impaired wound repair.
576 Pharmacol. Res. 58, 165–171.
577 Schiraldi, C., Alfano, A., Cimini, D., Rosa, M. D., Panariello, A., Restaino, O. F., Rosa, M.
578 D., 2012. Application of a 22L scale membrane bioreactor and cross‐flow
579 ultrafiltration to obtain purified chondroitin. Biotechnol. Progr., 28, 1012–1018.
580 Schmittgen, T. D., Livak, K. J., 2008. Analyzing real-time PCR data by the comparative CT
581 method. Nat. Protoc. 3, 1101–1103.
582 Shang, Q., Shi, J., Song, G., Zhang, M., Cai, C., Hao, J., Li, G., Yu, G., 2016. Structural
583 modulation of gut microbiota by chondroitin sulfate and its oligosaccharide. Int. J. of
584 Boil. Macromol. 89, 489–498.
585 Shen, W., Matsui, T., 2017. Current knowledge of intestinal absorption of bioactive peptides.
586 Food Funct. 8, 4306–4314.
587 Sun, H., Qi, D., Xu, Juan, J., S., Zhe, C., 2011. Fractionation of polysaccharides from

588 rapeseed by ultrafiltration: Effect of molecular pore size and operation conditions on the
589 membrane performance. Sep. Purify. Technol. 80, 670–676.
590 Takagi, H., Asano, Y., Yamakawa, N., Matsumoto, I., Kimata, K., 2002. Annexin 6 is a
591 putative cell surface receptor for chondroitin sulfate chains. J. Cell Sci. 115, 3309–3318.
592 Tao, J., Zhao, Y. Q., Chi, C. Wang, F., B., 2018. Bioactive peptides from cartilage protein
593 hydrolysate of spotless smoothhound and their antioxidant activity *in vitro*. Mar. Drugs.
594 16, 100–118.
595 Taye, N., Karoulias, S. Z., Hubmacher, D., 2020. The "other" 15–40%: the role of non-
596 collagenous extracellular matrix proteins and minor collagens in tendon. J. Orthop. Res.
597 38, 23–35.
598 Vázquez, J. A., Rodríguez-Amado, I., Montemayor, M. I., Fraguas, J., González, M. D. P.,
599 Murado, M. A., 2013. Chondroitin sulfate, hyaluronic acid and chitin/chitosan
600 production using marine waste sources: Characteristics, applications and eco-friendly
601 processes: A review. Mar. Drugs. 11, 747–774.
602 Volpi, N., 2007. Analytical aspects of pharmaceutical grade chondroitin sulfates. J. Pharm.
603 Sci. 96, 3168–3180.
604 Wang, L., Jiang, Y., Wang, X., Zhou, J., Cui, H., Xu, W., He, Y., Ma, H., Gao, R., 2018. Effect
605 of oral administration of collagen hydrolysates from Nile tilapia on the chronologically
606 aged skin. J. Funct. Foods, 44, 112–117.
607 Wu, F., Zhou, C., Zhou, D., Ou, S., Liu, Z., Huang, H., 2018. Immune-enhancing activities of
608 chondroitin sulfate in murine macrophage RAW 264.7 cells. Carbohyd. Polym. 168,
609 611–619.

610 Yoshimoto, M., Heike, T., Chang, H., Kanatsu-Shinohara, M., Baba, S., Varnau, J. T.,
611 Shinoharac, T., Yoder, M. C., Nakahata, 2009. T., Bone marrow engraftment but limited
612 expansion of hematopoietic cells from multipotent germline stem cells derived from
613 neonatal mouse testis. Exp. Hematol. 37, 1400–1410.
614 Zague, V., do Amaral, J. B., Rezende Teixeira, P., de Oliveira Niero, E. L., Lauand, C.,
615 Machado-Santelli, G. M., 2018. Collagen peptides modulate the metabolism of
616 extracellular matrix by human dermal fibroblasts derived from sun-protected and sun-
617 exposed body sites. Cell Biol. Int. 42, 95–104.
618 Zeng, Q., Fan, X., Zheng, Q., Wang, J., Zhang, X., 2018. Anti-oxidant, hemolysis inhibition,
619 and collagen-stimulating activities of a new hexapeptide derived from *Arthrospira*
620 (*Spirulina*) *platensis*. J. Appl. Phycol. 30, 1655–1665.
621 Zheng, L., Wei, H., Yu, H., Xing, Q., Zou, Y., Zhou, Y., Peng, J., 2018. Fish skin gelatin
622 hydrolysate production by ginger powder induces glutathione synthesis to prevent
623 hydrogen peroxide induced intestinal oxidative stress via the Pept1-p62-Nrf2 cascade. J.
624 Agr. Food. Chem. 66, 11601–11611.
625 Zou, T. B., He, T. P., Li, H. B., Tang, H. W., Xia, E. Q., 2016. The structure-activity
626 relationship of the antioxidant peptides from natural proteins. Molecules. 21, 72–86.
627 Zou, X. H., Jiang, Y. Z., Zhang, G. R., Jin, H. M., Hieu, N. T. M., Ouyang, H. W., 2009.
628 Specific interactions between human fibroblasts and particular chondroitin sulfate
629 molecules for wound healing. Acta Biomater. 5, 1588–1595.
630

631 **Figure captions**

632 **Fig. 1.** ABTS (A) and DPPH (B) radical scavenging activities of the by-product of skate
633 chondroitin sulfate production (BP-sCS), the papain-hydrolyzed type II collagen peptides
634 (Pa-CP), and the chondroitin sulfate polysaccharides (CSp). Values have been expressed as
635 the mean ± standard error (n = 3).

636

637 **Fig. 2.** ABTS radical scavenging activities (A) and molecular weight distributions (B) of
638 <3000 Da fractions of the by-product of skate chondroitin sulfate production (BP-sCS) and
639 the papain-hydrolyzed type II collagen peptides (Pa-CP). BP-sCS <3, BP-sCS fraction of less
640 than 3000 Da; Pa-CP <3, Pa-CP fraction of less than 3000 Da. Columns and bars indicate the
641 mean value ± standard error (n = 3). ** p <0.01, the Student's t-test.

642

643 **Fig. 3.** Effects of the by-product of skate chondroitin sulfate production (BP-sCS), the
644 papain-hydrolyzed type II collagen peptides (Pa-CP), and the chondroitin sulfate
645 polysaccharides (CSp) against (A) H_2O_2- and (B) AAPH-induced oxidative stress on the
646 L929 fibroblast proliferation/metabolism. Control groups were not treated with oxidants.
647 Oxidative stress was induced in all other groups using H_2O_2 (A) or AAPH (B). Sample
648 concentration, 1 mg/mL. EFW, endotoxin-free water. Columns and bars indicate the mean
649 value ± standard error (n = 12–16). # p <0.05, ## p <0.01 compared to the control group (the
650 Steel-Dwass test). Different letters denote significant differences between groups (p <0.05,
651 the Steel-Dwass test).

652

653 **Fig. 4.** Effects of the by-product of skate chondroitin sulfate production (BP-sCS), the
654 papain-hydrolyzed type II collagen peptides (Pa-CP), and the chondroitin sulfate
655 polysaccharides (CSp) on the H_2O_2-induced intracellular ROS production. Control groups
656 were not treated with H_2O_2. Oxidative stress was induced in all other groups using 0.5 mM
657 H_2O_2. EFW, endotoxin-free water; VC, Vitamin C 0.2 mg/mL; BP-sCS 0.01, BP-sCS 0.01
658 mg/mL; BP-sCS 0.1, BP-sCS 0.1 mg/mL; BP-sCS 1, BP-sCS 1 mg/mL; Pa-CP 0.01, Pa-CP
659 0.01 mg/mL; Pa-CP 0.1, Pa-CP 0.1 mg/mL; Pa-CP 1, Pa-CP 1 mg/mL; CSp 0.01, CSp 0.01
660 mg/mL; CSp 0.1, CSp 0.1 mg/mL; CSp 1, CSp 1 mg/mL. Columns and bars indicate the
661 mean value ± standard error (n = 9–10). Different letters denote significant differences
662 between groups (p <0.05, the Steel-Dwass test).

663

664 **Fig. 5.** Effect of the by-product of skate chondroitin sulfate production (BP-sCS), the papain-
665 hydrolyzed type II collagen peptides (Pa-CP), and the chondroitin sulfate polysaccharides
666 (CSp) on the L929 fibroblast proliferation/cell metabolism. Values have been expressed
667 relative to the corresponding endotoxin-free water (EFW) control. BP-sCS 0.01, BP-sCS
668 0.01 mg/mL; BP-sCS 0.1, BP-sCS 0.1 mg/mL; BP-sCS 1, BP-sCS 1 mg/mL; Pa-CP 0.01, Pa-
669 CP 0.01 mg/mL; Pa-CP 0.1, Pa-CP 0.1 mg/mL; Pa-CP 1, Pa-CP 1 mg/mL; CSp 0.01, CSp
670 0.01 mg/mL; CSp 0.1, CSp 0.1 mg/mL; CSp 1, CSp 1 mg/mL. Columns and bars indicate the
671 mean value ± standard error (n = 6). Different letters denote significant differences between
672 groups (p <0.05, the Steel-Dwass test).

673

674 **Fig. 6.** Effect of the by-product of skate chondroitin sulfate production (BP-sCS), the papain-
675 hydrolyzed type II collagen peptides (Pa-CP), and the chondroitin sulfate polysaccharides
676 (CSp) on collagen mRNA expression (A) and the amount of collagen secreted into the culture
677 medium or the extracellular matrix (ECM) (B) by the L929 fibroblasts. The collagen mRNA
678 expression levels have been normalized to the internal control (*Gapdh*) and expressed relative
679 to the corresponding endotoxin-free water (EFW) control. Sample concentration, 1 mg/mL.
680 Columns and bars indicate the mean value ± standard error (n = 11–12 in A and n = 6 in B). *
681 p <0.05, compared to the EFW control group (the Dunnett's test). ** p <0.01, Student's t-test.

682

683 **Fig. 7.** Effect of the by-product of skate chondroitin sulfate production (BP-sCS), the papain-
684 hydrolyzed type II collagen peptides (Pa-CP), and the chondroitin sulfate polysaccharides
685 (CSp) on the L929 fibroblast migration. (A) The scratch assay without oxidative stress.
686 Samples concentration, 1 mg/mL. Values have been expressed as the mean ± standard error (n
687 = 5–6). # p <0.05 compared to the control group (the Dunnett's test). (B, C) The scratch assay
688 under the oxidative stress. The control group was not treated with AAPH. Other groups were
689 treated with 5.0 mM (B) or 2.5 mM (C) AAPH. Samples concentration, 1 mg/mL. Values
690 have been expressed as the mean ± standard error (n = 5–6). # p <0.05 compared to the
691 control group (the Dunnett's test). *p <0.05 compared to the endotoxin-free water (EFW)
692 group (the Dunnett's test). (D) Photomicrographs of the L929 fibroblasts at 48 h in the scratch
693 assay under the oxidative stress. Samples concentration, 1 mg/mL. Bars, 250 μm in photos
694 and enlarged photos.

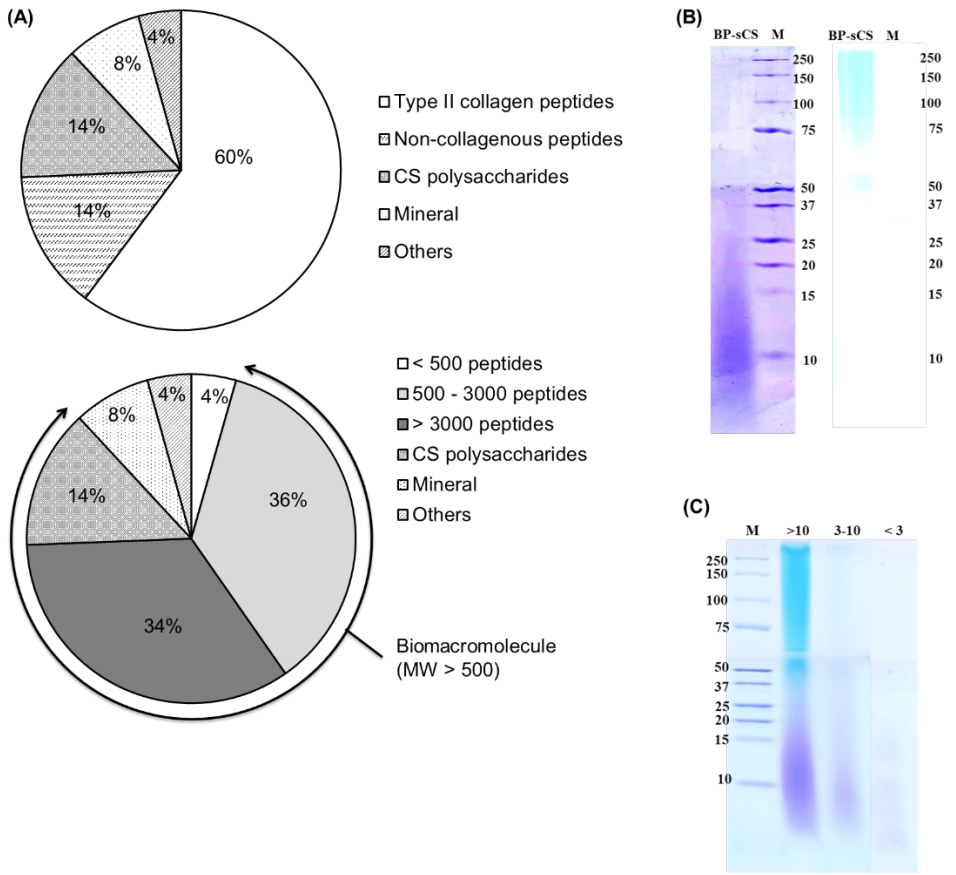

Supplementary Fig.1. Composition of the by-product of skate chondroitin sulfate (BP-sCS)

(A) BP-sCS contains CS polysaccharides, peptides, minerals and others (lipid, water, and so on). The lower graph showed the molecular weight distribution of peptides.

(B) Tricine-SDS-PAGE of BP-sCS with Coomassie Brilliant Blue (CBB) (left) and Alcian blue (right) stains. CBB and Alcian blue stains showed peptides and CS polysaccharides in BP-sCS, respectively. M, protein markers.

(C) Tricine-SDS-PAGE of BP-sCS separated by ultrafiltration membrane. Samples were stained with CBB and Alcian blue. CBB and Alcian blue stains showed peptides and CS polysaccharides in different fractions of BP-sCS, respectively. < 3000 Da fraction was negative

to Alcian blue stain, suggesting it contains no CS. M, protein markers; >10, BP-sCS fraction of more than 10000 Da; 3–10, BP-sCS fraction of between 3000–10000 Da; < 3, BP-sCS fraction of smaller than 3000 Da.

Supplementary Table 1

The formulations and molecular weights of CSp

	Formulations (%)					Molecular weight (kDa)
	ΔDi-0s	ΔDi-4s (CS-A)	ΔDi-6s (CS-C)	ΔDi-2,6s (CS-D)	ΔDi-4,6s (CS-E)	
CSp	6.5	26.6	60.9	6.5	0.1	37–250

Data of formulations for CSp were obtained by Marukyo Bio Foods Co. Ltd. Data of molecular weights were obtained by 16.5% tricine-SDS-PAGE stained with Alcian blue.

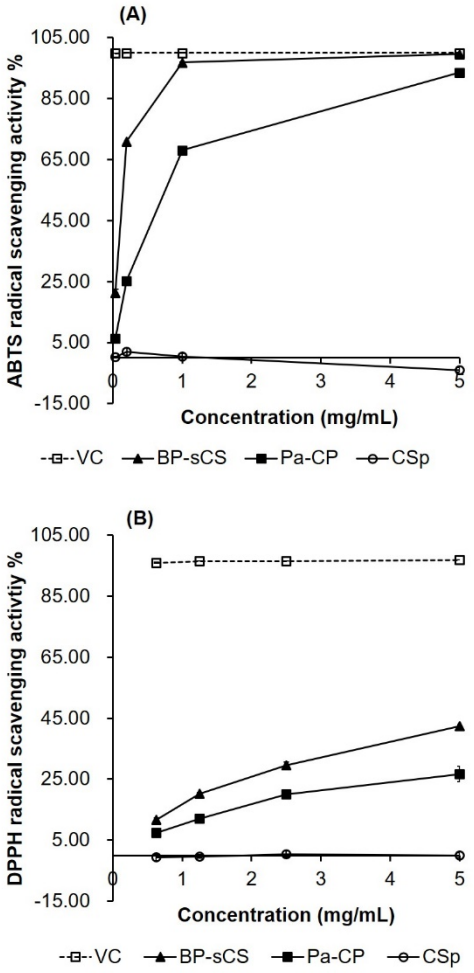
(A)
105.00
85.00
65.00
45.00
25.00
5.00
-15.00
ABTS radical scavenging activity %
0
1
2
3
4
5
Concentration (mg/mL)
VC
BP-sCS
Pa-CP
CSp
(B)
105.00
85.00
65.00
45.00
25.00
5.00
-15.00
DPPH radical scavenging activtiy %
0
1
2
3
4
5
Concentration (mg/mL)
VC
BP-sCS
Pa-CP
CSp

Fig. 1

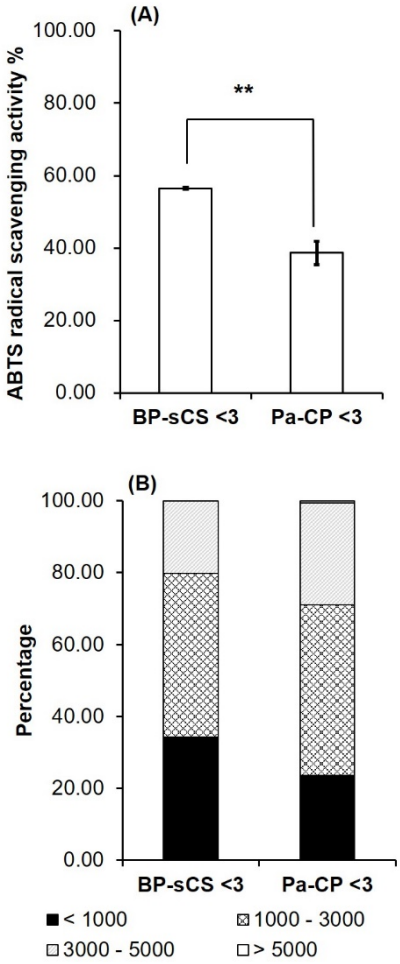
(A)
ABTS radical scavenging activity %
100.00
80.00
60.00
40.00
20.00
0.00
**
BP-sCS <3
Pa-CP <3
(B)
Percentage
100.00
80.00
60.00
40.00
20.00
0.00
BP-sCS <3
Pa-CP <3
< 1000
1000 - 3000
3000 - 5000
> 5000

Fig. 2

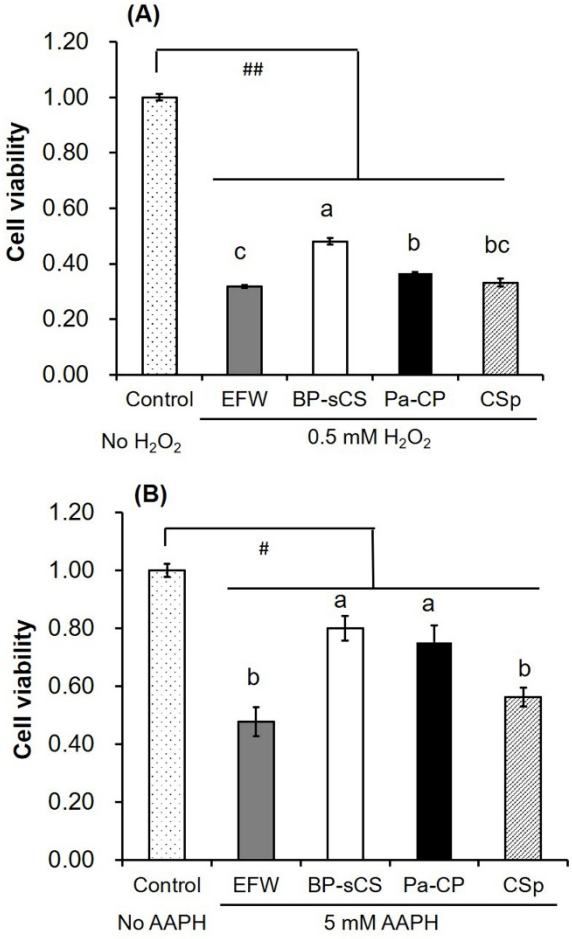
(A)
1.20
1.00
0.80
0.60
0.40
0.20
0.00
Cell viability
##
a
c
b
bc
Control
EFW
BP-sCS
Pa-CP
CSp
No H_2O_2
0.5 mM H_2O_2
(B)
1.20
1.00
0.80
0.60
0.40
0.20
0.00
Cell viability
#
a
a
b
b
Control
EFW
BP-sCS
Pa-CP
CSp
No AAPH
5 mM AAPH

Fig. 3

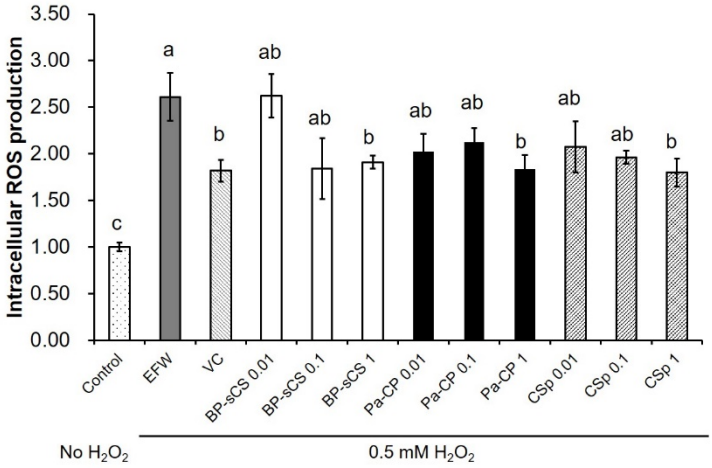
Intracellular ROS production
3.50
3.00
2.50
2.00
1.50
1.00
0.50
0.00
c
a
b
ab
ab
b
ab
ab
b
ab
ab
b
Control
EFW
VC
BP-sCS 0.01
BP-sCS 0.1
BP-sCS 1
Pa-CP 0.01
Pa-CP 0.1
Pa-CP 1
CSp 0.01
CSp 0.1
CSp 1
No H_2O_2
0.5 mM H_2O_2

Fig. 4

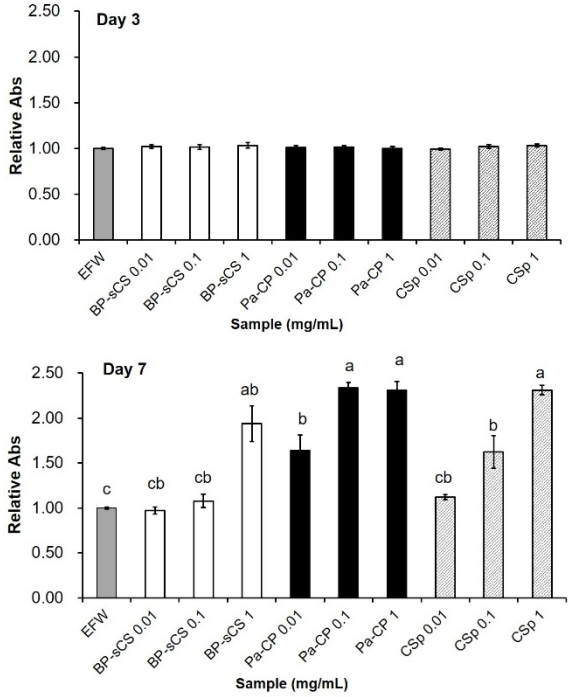
Day 3
Relative Abs
2.50
2.00
1.50
1.00
0.50
0.00
EFW
BP-sCS 0.01
BP-sCS 0.1
BP-sCS 1
Pa-CP 0.01
Pa-CP 0.1
Pa-CP 1
CSp 0.01
CSp 0.1
CSp 1
Sample (mg/mL)
Day 7
Relative Abs
c
cb
cb
ab
b
a
a
cb
b
a
Sample (mg/mL)

Fig. 5

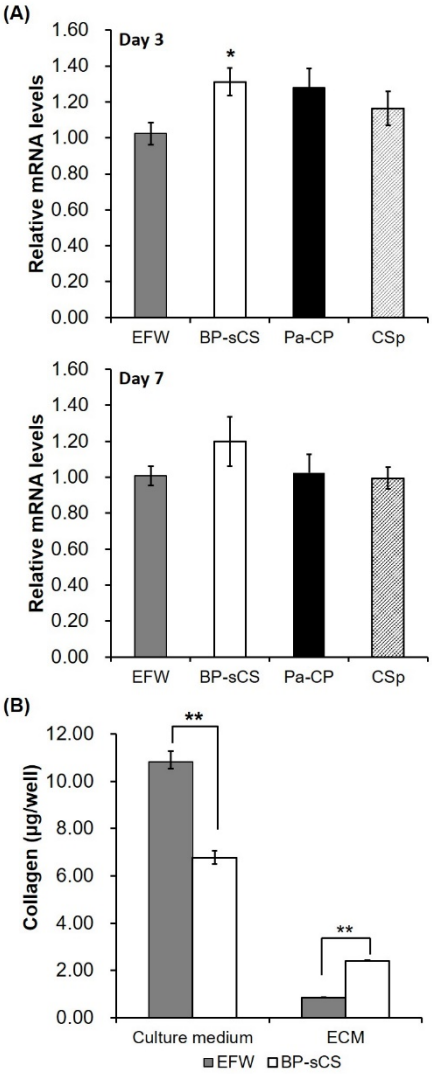
(A)
Day 3
Relative mRNA levels
1.60
1.40
1.20
1.00
0.80
0.60
0.40
0.20
0.00
*
EFW
BP-sCS
Pa-CP
CSp
Day 7
Relative mRNA levels
1.60
1.40
1.20
1.00
0.80
0.60
0.40
0.20
0.00
EFW
BP-sCS
Pa-CP
CSp
(B)
Collagen (μg/well)
12.00
10.00
8.00
6.00
4.00
2.00
0.00
**
**
Culture medium
ECM
EFW
BP-sCS

Fig. 6

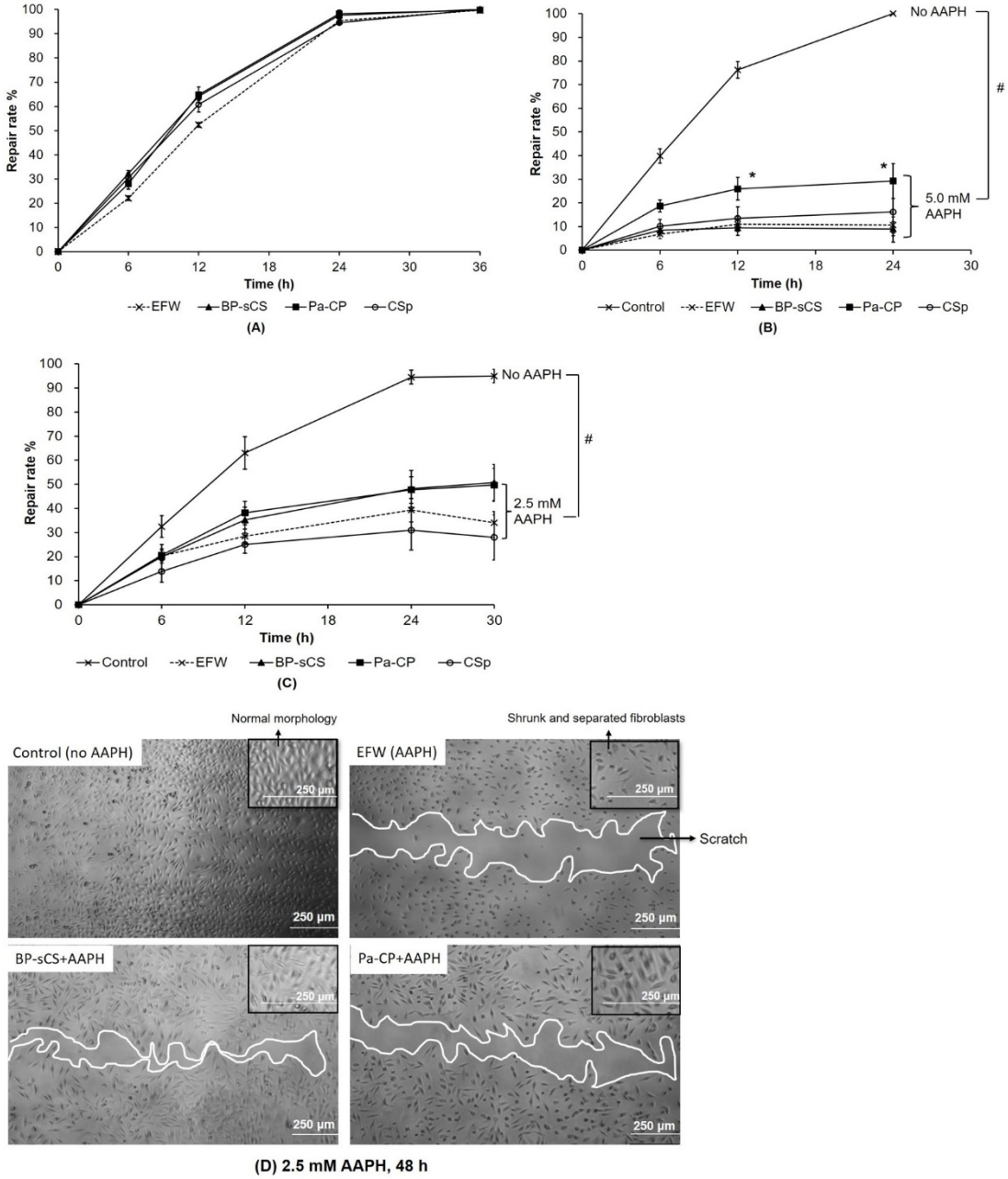
Repair rate %
Time (h)
EFW
BP-sCS
Pa-CP
CSp
(A)
No AAPH
5.0 mM AAPH
#
*
Control
(B)
2.5 mM AAPH
(C)
Normal morphology
Shrunk and separated fibroblasts
Control (no AAPH)
EFW (AAPH)
Scratch
BP-sCS+AAPH
Pa-CP+AAPH
250 µm
(D) 2.5 mM AAPH, 48 h

Fig. 7